

MPI-PhT/97-46
July 18, 1997

Unified QCD Description of Hadron and Jet Multiplicities

Sergio Lupia* and Wolfgang Ochs†

*Max-Planck-Institut für Physik, (Werner-Heisenberg-Institut)
Föhringer Ring 6, 80805 München, Germany*

Abstract

The evolution equation for parton multiplicities in quark and gluon jets which takes into account the soft gluon interference is solved numerically using the initial conditions at threshold. If the k_\perp -cutoff Q_c is lowered towards the hadronic scale Q_0 of a few hundred MeV, the jets are fully resolved into hadrons. Both hadron and jet multiplicities in e^+e^- annihilation are well described with a common normalization. Evidence is presented within this perturbative approach that the coupling $\alpha_s(k_\perp)$ rises by an order of magnitude when approaching the low energy region. The ratio of hadron multiplicities in gluon and quark jets is found smaller than in previous approximate solutions of the evolution equation.

*E-mail address: lupia@mppmu.mpg.de

†E-mail address: wwo@mppmu.mpg.de

1 Introduction

One of the simplest characteristics of the hadronic final state is the particle multiplicity. Following the ideas of a soft hadronization mechanism [1,2] the observable hadron multiplicity in a quark or gluon jet is expected to follow closely that of the final QCD partons in its energy dependence. More specifically, within the picture of local parton hadron duality (LPHD) [3] the primary parton of energy E generates a parton cascade which is evolved down to small scales of a few hundred MeV for the transverse momentum cutoff Q_0 . Then, within the so-called modified leading logarithmic approximation (MLLA), which takes into account the leading double logarithmic and next to leading single logarithmic terms, a good description of the mean charged particle multiplicity in e^+e^- annihilation as a function of the primary *cms* energy $\sqrt{s} \equiv Q = 2E$ is obtained with a formula

$$\mathcal{N}_{ch}^{e^+e^-}(Q) = 2K_{ch}\mathcal{N}_q\left(\frac{Q}{Q_0}, \frac{Q_0}{\Lambda}\right) + \text{const.} \quad (1)$$

Here \mathcal{N}_q denotes the multiplicity of partons in a single quark jet of energy E and Λ is the QCD scale. From fits in the energy range $Q = 3\dots 160$ GeV one typically finds $Q_0 \gtrsim \Lambda \approx 250$ MeV and the normalization $K_{ch} \approx 1.2$ [3,4,5]. Assuming $K_{ch} = \frac{2}{3}K_{all}$ the number of all hadrons (charged and neutral) is then about twice as large as the number of partons ($K_{all} \approx 2$).

Another characteristic of the final state is the mean multiplicity of jets $\mathcal{N}_{jet}(Q_c, Q)$ for a given resolution parameter Q_c , or, in conventional normalization, $y_c = Q_c^2/Q^2$. Early results at low resolution in $\mathcal{O}(\alpha_s^2)$ [6] played an important role as a QCD test and in the determination of the running coupling α_s . The calculation of jet multiplicities to all orders in α_s became feasible using the Durham/ k_\perp algorithm [7] which takes as separation parameter for two jets the measure

$$y_{ij} = 2 \min(E_i^2, E_j^2) \frac{1 - \cos \Theta_{ij}}{Q^2} \quad (2)$$

which for small relative angles Θ_{ij} approximates the rescaled transverse momentum $(k_\perp^{ij})^2/Q^2$ of the jet of lower momentum with respect to that of higher momentum. Then the jet multiplicity $\mathcal{N}_{jet}(y_c, Q)$ refers to all jets with separation $y_{ij} \geq y_c$. Jet multiplicities in leading and next-to-leading order of $\ln y_c$ have been calculated [8,9,10,11] and, after matching with the full $\mathcal{O}(\alpha_s^2)$ results, a good description of jet multiplicities down to $y_c \sim 10^{-3}$ has been obtained [12,13]. In these calculations the jet multiplicities are derived in absolute normalization ($K_{all} = 1$) from

$$\mathcal{N}_{jet}^{e^+e^-}(Q_c, Q) = 2\mathcal{N}_q\left(\frac{Q}{Q_c}, \frac{Q_c}{\Lambda}\right). \quad (3)$$

In this paper we investigate whether both observables, jet multiplicities and hadron multiplicities, can be described in a unified way. Indeed, the resummation of the perturbative series has been achieved in both cases by using the same type of evolution equation. Also, the Durham/ k_\perp algorithm of the jet definition (2) coincides for $Q_c \rightarrow Q_0$ with the prescription $k_\perp \geq Q_0$ which is applied in the description of hadrons within the LPHD picture. At a first sight there is no smooth transition for $Q_c \rightarrow Q_0$ from (3) to (1) because of the two additional constants in (1). Furthermore, various jet observables for small y_c deviate from the perturbative predictions (see, for example, review [14]), and this is often taken as evidence for nonperturbative hadronization effects at the resolution scales $Q_c \sim 1 - 2$ GeV.

We show that these problems – in the case of the mean jet or particle multiplicity – disappear if the underlying coupled evolution equations for quark and gluon jets are solved with sufficiently high accuracy; here we perform a numerical integration to obtain the exact solutions.

2 Evolution equation for multiplicities

We start from the evolution equation for the generating functional of the multiparton final state [15,2] which, in the parton splitting process $A \rightarrow B+C$, takes into account angular ordering, energy conservation and the running coupling at the one-loop order. By appropriate differentiation we obtain the evolution equations for the mean parton multiplicities \mathcal{N}_q and \mathcal{N}_g in quark and gluon jets with jet virtuality κ (see also [11]) or with

$$\eta = \ln \frac{\kappa}{Q_c}, \quad \kappa = Q \sin \frac{\Theta}{2}. \quad (4)$$

where Θ denotes the maximum angle between the outgoing partons B and C . At fixed cutoff Q_c these equations read

$$\begin{aligned} \frac{d\mathcal{N}_g(\eta)}{d\eta} &= \int_{z_c}^{1-z_c} dz \frac{\alpha_s(\tilde{k}_\perp)}{2\pi} [\Phi_{gg}^{asy}(z) \{\mathcal{N}_g(\eta + \ln z) + \mathcal{N}_g(\eta + \ln(1-z)) - \mathcal{N}_g(\eta)\} \\ &\quad + n_f \Phi_{gq}(z) \{\mathcal{N}_q(\eta + \ln z) + \mathcal{N}_q(\eta + \ln(1-z)) - \mathcal{N}_q(\eta)\}] \\ \frac{d\mathcal{N}_q(\eta)}{d\eta} &= \int_{z_c}^{1-z_c} dz \frac{\alpha_s(\tilde{k}_\perp)}{2\pi} \Phi_{gq}(z) \{\mathcal{N}_g(\eta + \ln z) + \mathcal{N}_q(\eta + \ln(1-z)) - \mathcal{N}_q(\eta)\}. \end{aligned} \quad (5)$$

The splitting functions Φ_{AB} for parton splitting $A \rightarrow B$ [16] are taken with normalization as in [2], i.e., $\Phi_{gg}(z) \simeq 4N_c/z$ at small z (N_C and n_f denote the number of colours and flavours). Because of its symmetry property it is convenient to replace $\frac{1}{2}\Phi_{gg}(z)$ by the asymmetric function $\Phi_{gg}^{asy}(z) = (1-z)\Phi_{gg}(z)$ in (5) [11].

The boundaries of the integral over the parton momentum fractions z are determined by the lower cutoff in the transverse momentum measure \tilde{k}_\perp defined according to (2) with the approximation $z_A \approx 1 - z_B$

$$\tilde{k}_\perp = \min(z, 1 - z)\kappa \geq Q_c. \quad (6)$$

The lower bound z_c in (5) is obtained for minimal $z = Q_c/(Q \sin \frac{\Theta}{2})$ which is found for $\Theta \approx \frac{\pi}{2}$ (in this configuration, because of transverse momentum conservation, the high energy secondary parton has production angle $\vartheta_A \approx 0$ and the soft particle $\vartheta_B \lesssim \frac{\pi}{2}$); more generally, Θ corresponds to the half opening angle of the jet ($\vartheta_B \leq \Theta$). Therefore z_c is given by

$$z_c = \frac{Q_c \sqrt{2}}{Q} = \sqrt{2y_c} = e^{-\eta}. \quad (7)$$

Since $z_c \leq \frac{1}{2}$, one finds $y_c \leq \frac{1}{8}$ and $\eta \geq \ln 2$.

The coupling is given by $\alpha_s(\tilde{k}_\perp, n_f) = 2\pi/(b \ln(\tilde{k}_\perp/\Lambda))$ with $b = (11N_C - 2n_f)/3$. We evolve $\alpha_s(\tilde{k}_\perp, n_f)^{-1}$ with \tilde{k}_\perp by matching smoothly the couplings for n_f and $n_f + 1$ at twice the heavy quark thresholds according to the formula

$$\frac{1}{\alpha_s(k_t)} = \frac{\Theta(k_t - 2m_{n_f})}{\alpha_s^{(n_f)}(k_t)} - \sum_{i=4}^{n_f} \left(\frac{1}{\alpha_s^{(i)}(m_i)} - \frac{1}{\alpha_s^{(i-1)}(m_i)} \right) \Theta(k_t - 2m_i) \quad (8)$$

The factor two in the threshold for heavy quark production takes into account that heavy quarks are produced in pairs by a gluon.

The differential equations are defined only for $\eta \geq \ln 2$. The initial conditions for the solutions of (5) then read (for any fixed Q_c)

$$\mathcal{N}_g(\eta) = \mathcal{N}_q(\eta) = 1 \quad \text{for } 0 \leq \eta \leq \ln 2. \quad (9)$$

Analytical solutions using the boundary conditions at threshold have been derived within the MLLA for gluon jets[17] and for the coupled system of quark and gluon jets[10]. Whereas the MLLA yields a good high energy behaviour, it leads to inconsistencies ($\mathcal{N}'_a(\eta) < 0$) near threshold. In the present analysis we solve the equations (5) and (9) numerically.¹

The two jets in e^+e^- annihilation evolve independently in this approximation. Near threshold this factorization of the generating functional does not

¹We start from $\mathcal{N}_a(\eta = \ln 2) = 1$, calculate $\mathcal{N}_a(\eta + \delta\eta)$ in steps of length $\delta\eta$ from the derivatives (5) as $\mathcal{N}'_a(\eta)\delta\eta$ using the trapezoidal rule for the integration and linear interpolation for the required \mathcal{N} values under the integral. The integration is performed with logarithmic variable $y = \ln z$.

hold any more and non-logarithmic terms become important. For the k_\perp resolution criterion (2) the inelastic threshold is found for symmetric 3-jet events ($\Theta = \frac{2\pi}{3}$, $z = \frac{2}{3}$) with $y_c = \frac{1}{3}$ or $\eta = \frac{1}{2} \ln \frac{3}{2}$. This is to be compared with $y_c = \frac{1}{8}$ and $\eta = \ln 2$ for eq. (5). The difference of thresholds will clearly affect the results in the large y_c region.

An improvement in this region can be achieved by replacing the contribution of $\mathcal{O}(\alpha_s)$ in (5) by the explicit result for $e^+e^- \rightarrow 3$ partons in $\mathcal{O}(\alpha_s)$ (see also Ref. [10,8]). The lowest order contribution $\mathcal{N}_q^{(1)}$ of the evolution equation is obtained by taking the first iteration of (5) with the initial conditions (9), i.e., replacing the three \mathcal{N} -terms in the curly brackets in (5) by unity. The full $\mathcal{O}(\alpha_s)$ contribution is found by numerical integration of

$$\mathcal{N}^{3-jet}(y_c) = 2 \int_{1/2}^1 dz_1 \int_{1-z_1}^{z_1} dz_2 \Theta(d_{23} - y_c) \frac{C_F \alpha_s(\tilde{k}_\perp)}{2\pi} \frac{z_1^2 + z_2^2}{(1-z_1)(1-z_2)} \quad (10)$$

$$d_{23} = \min \left(\frac{z_2}{z_3}, \frac{z_3}{z_2} \right) (1-z_1) > y_c \quad (11)$$

where z_1 (z_2) denote the quark (antiquark) and $z_3 = 2 - z_1 - z_2$ the gluon momentum fractions ($C_F = 4/3$). Here the coupling is taken again as running with the k_\perp measure (2) $\tilde{k}_\perp = (d_{23} Q^2)^{\frac{1}{2}}$ as scale in the integration region $z_2 < z_1$ in (10). The $\mathcal{O}(\alpha_s)$ corrected solution $\mathcal{N}_{corr}^{e^+e^-}$ is then obtained from

$$\mathcal{N}_{corr}^{e^+e^-}(y_c) = 2\mathcal{N}_q(y_c) - 2\mathcal{N}_q^{(1)}(y_c) + \mathcal{N}^{3-jet}(y_c). \quad (12)$$

A corresponding improved result for the gluon jet is not yet available and has to be considered for each process separately. In this paper we apply the equation (12) to the full range of scale parameters $Q_0 < Q_c < Q$, i.e., we study the jet region ($y_c \gtrsim 0.01$) and also the transition from the jets to the fully resolved hadrons ($y_c \sim (Q_0/Q)^2$).

3 Confronting predictions with experiment

3.1 Multiplicities in e^+e^- annihilation

In Fig. 1a we show the data of the average jet multiplicity at $Q = 91$ GeV [12,13] as a function of the resolution parameter $y_c = Q_c^2/Q^2$ as obtained with the k_\perp algorithm. The theoretical predictions from (12) for the jet data are given in absolute normalization in terms of the single parameter Λ . Also shown are the data on hadron multiplicities in the energy range $Q = 1.6 \dots 91$ GeV [18] taken as $\mathcal{N}_{all} = \frac{3}{2} \mathcal{N}_{ch}$ as a function of the same scale parameter, now calculated as $y_c = Q_0^2/Q^2$, where the parameter Q_0 corresponds to the

parton k_\perp cutoff characterizing a hadronic scale and is obtained from a fit to the data. Another adjustable parameter here is the overall normalization K_{all} which relates the parton and hadron multiplicities in $\mathcal{N}_{all} = K_{all}\mathcal{N}_{corr}^{e^+e^-}$. We determine first the Λ parameter from the jet multiplicity (lower data set in Fig. 1) and then the K_{all} and Q_0 from the hadronic multiplicity (upper data set). A good description of the data is obtained with parameters

$$K_{all} = 1, \quad \Lambda = 500 \pm 50 \text{ MeV} \quad \lambda = \ln \frac{Q_0}{\Lambda} = 0.015 \pm 0.005 \quad (13)$$

which correspond to the curves shown in Fig. 1a. The quantity $\mathcal{N} - 2$ derived from the same experimental data is shown in Fig. 1b. The dashed curves represent the contribution $2\mathcal{N}_q$ in (12) from the evolution equation alone. The fits can be seen to describe quantitatively the hadron multiplicity, the jet multiplicity for the small and large y_c , whereas in the intermediate region around $y_c \simeq 0.01$ the fit exceeds the data on $\mathcal{N} - 2$ by up to 20% (up to 5% in \mathcal{N}). Deviations of this type may indicate the importance of two-loop $\mathcal{O}(\alpha_s^2)$ terms not included in the analysis.

As a remarkable result of our analysis we find that the common normalization $K_{all} = 1$ is possible without difficulty; the normalization parameter K_{all} is correlated with Q_0 and can be varied within about 30%. The solution with $K_{all} = 1$ is natural as it provides the correct boundary conditions $\mathcal{N} = 2$ at threshold for both hadrons and jets. Then a continuous connection between jet and hadron data results, since both are described by the same evolution equation (12). In this description a single hadron corresponds to a single parton of low virtuality Q_0 .

It is interesting to compare the two sets of data at the same y_c . The difference between the two curves comes entirely from the running of α_s . Namely, if α_s were kept fixed in equations (5) the resulting multiplicities would depend only on the ratio of the available scales through the variable $\eta = -\frac{1}{2}\ln(2y_c)$ but not on the absolute size of Q and the two curves in Fig. 1 would coincide. A model with fixed α_s would predict at high energy a power like dependence on Q , i.e. a straight line in Fig. 1a between the two curves shown.

The largest difference occurs near the inelastic threshold at $y_c \approx \frac{1}{8}$ or $\eta \approx \ln 2$. In this region $\mathcal{N} - 2$ is dominated by the contribution of order α_s and the jet and hadron results at the same y_c are in the ratio of the relevant typical coupling constants. At the lowest available energy for the hadron multiplicity ($y_c \sim 0.1$, $Q = 1.6$ GeV) this ratio of couplings is larger than 10, so the typical coupling to produce hadrons at 1.6 GeV is $\alpha_s \gtrsim 1$. The good matching of the prediction for hadrons with the boundary condition at threshold suggests that the coupling is rising even more towards lower energies. The

strong variation of the coupling at small scales has been found important also in the description of particle energy spectra[5,19]. On the other hand, the jet multiplicity is first rising very slowly with decreasing y_c , because of the small coupling ($\alpha_s \sim 0.1$). Only for very high resolution, if Q_c is lowered from 900 MeV ($y_c \sim 10^{-4}$) to the final 500 MeV, about three quarters of the final multiplicity are produced, three times as many jets as in the large complementary kinematic region. The steep rise toward small y_c in Fig. 1 reflects the singularity in the coupling at $y_\Lambda = \Lambda^2/Q^2$, which is however screened by the hadronization scale $y_0 = (Q_0)^2/Q^2 \gtrsim y_\Lambda$. This behaviour is qualitatively described by the high energy DLA result[2] $\mathcal{N} \sim K_0(A\sqrt{\lambda_c})I_1(A\sqrt{\ln(\kappa/\Lambda)}) + \dots$ with $A = \sqrt{16N_C/b}$ which at high energies and small $\lambda_c = \ln(Q_c/\Lambda)$ behaves as $\ln \lambda_c \exp(A\sqrt{\ln(\kappa/\Lambda)})$. This form, for fixed Q_c , describes the slow rise of multiplicity with $\kappa \sim Q$, whereas, for fixed Q , it exhibits the logarithmic singularity for $\lambda_c \rightarrow 0$. This singularity arises in the first iteration of (5) (the “Born-term”) from the contribution $\int_0^\eta dy/(y + \lambda)$.

Previous approximate solutions had been restricted to $y_c \gtrsim 0.002$ for jets, whereas for hadrons the analytical results could only be applied to the higher energy region with a larger K_{ch} factor.² Our results are consistent with the previous finding $\lambda \lesssim 0.1$ from the energy moments [5]; on the other hand, $\lambda = 0$ is not allowed in (5), as the multiplicity would diverge in this case.

It will be interesting to study this behaviour further near the transition $Q_c \rightarrow Q_0$ also at other *cms* energies, especially for the jet multiplicity, since it varies strongly in the low y_c range. In the experimental analysis using eq. (2) the full hadronic multiplicity will only be reached for $y_c \rightarrow 0$. The same lower cutoff for partons and hadrons is achieved if we interpret Q_c as transverse mass cutoff with Q_0 as effective mass parameter (see also [5,19]), i.e., if we relate the theoretical predictions and experimental results from cutoff (2) by $y_c^{th} = y_c^{exp} + Q_0^2/Q^2$.

The value (13) for the scale Λ is larger than that found in previous analyses of particle spectra[3,4,5]. This difference comes from taking the Durham \tilde{k}_\perp not only in the integral boundaries but also as argument of α_s and in the definition of hadrons by $\tilde{k}_\perp \geq Q_0$. We performed an alternative calculation where we used the standard $k_\perp < \tilde{k}_\perp$ as argument of α_s (i.e., $k_\perp = z(1-z)\kappa$ instead of eq. (6) and the exact k_\perp in eq. (10)) and inserted the cutoff $\Theta(k_\perp - Q_0)$ into eqs. (5) and (10); then a description of comparable quality is obtained

²The different value of the normalization factor as compared to previous analyses (for example [3,4,5]) is due to the use in the MLLA approximation of the initial conditions which have negative slope $\mathcal{N}'(\eta = 0) < 0$ and therefore lead to a delayed rise with energy [10]. Our exact solution in the present *cms* energy range is about twice as large and rises more slowly than the analytical MLLA solution for $Q_0 = \Lambda$ [17].

with the lower scale $\Lambda \sim 0.35$ GeV and the same λ parameter³. The threshold for hadrons is shifted in this case to the lower value $y_c = 1/12$ and also the hadron data points are shifted to the left in Fig. 1 according to the lower value of Q_0 . Our conclusions about the order of magnitude variation of α_s remain unaltered. The ambiguity in choosing the scale for α_s may be reduced in 2-loop calculations; for now we stay with the conceptually simplest possibility and take \tilde{k}_\perp throughout.

3.2 Multiplicities in gluon jets

The evolution equations (5) yield also results on the mean multiplicity \mathcal{N}_g in gluon jets. The results derived here refer to the multiplicity in the full hemisphere of the gluon jet and can be measured, for example, in a final state with a primary gg colour singlet state. Such a state is expected to be produced in the decay of heavy quarkonia; recently the multiplicity in the decay $Y \rightarrow gg\gamma$ has been measured by the CLEO Collaboration [20]. An initial state of this type can also be realized approximately in $e^+e^- \rightarrow 3$ jets with nearly antiparallel q and \bar{q} recoiling against the gluon [2,21]; this configuration has been analysed by the OPAL Collaboration [22]⁴. Our results do not apply immediately to other configurations (like “Y” or “Mercedes”) where the large angle soft radiation from the gluon is suppressed (for reviews, see [23,14]).

Of special interest is the ratio of gluon and quark jet multiplicity $r = \mathcal{N}_g/\mathcal{N}_q$, which is predicted to approach asymptotically the value $r = \frac{9}{4}$ [24]. The next-to-leading order corrections decrease this ratio at finite energies [25] and yet further with the inclusion of higher order corrections [26,27]. There is an uncertainty with these asymptotic predictions in that the region of validity is not known a priori. A complete solution of the evolution equations (5) requires an initial value for the multiplicities at some energy. Such results with absolute normalization at threshold have been presented within the MLLA [10].

We have obtained the results from our evolution equation (5) with initial condition (9), however, we have not yet included a low energy correction term as in (12) which is beyond the scope of this paper. The results for the ratio r are shown in Fig. 2 again as function of $y_c = (Q_c/Q)^2$ for hadron multiplicities in comparison with the OPAL and CLEO data mentioned above. Also shown is the prediction for jets at fixed $Q = 91$ GeV which could be tested using the same type of events with antiparallel $q\bar{q}$.

³The remaining difference to the earlier $\Lambda \simeq 250$ GeV comes from taking the scale $\kappa = \sqrt{2}E$ in (6) instead of $\kappa = E$.

⁴The full multiplicity in the hemisphere opposite to $q\bar{q}$ corresponding to our calculation is obtained if the higher jet multiplicities are also taken into account.

There is a very good agreement of our calculation with the OPAL data which refer to jet energies of ~ 40 GeV. From Fig. 1b one may expect that the inclusion of the full $\mathcal{O}(\alpha_s)$ corrections would not modify the prediction essentially (by more than about 10%). On the other hand, the CLEO data fall considerably below the prediction $r \sim 1.25$ from the evolution equation. In this region, however, the low energy corrections may not be small: in Fig 1b these corrections correspond to a factor of two. A more precise prediction of the Y data will require the inclusion of the full $\mathcal{O}(\alpha_s)$ correction to the $Y \rightarrow gg\gamma$ process.

4 Conclusions

We solved the QCD evolution equations for quark and gluon jets exactly by numerical integration and also supplemented the full $\mathcal{O}(\alpha_s)$ correction for e^+e^- annihilation. With this improved accuracy beyond MLLA we obtain a unified description with common absolute normalization of the mean jet multiplicity at LEP-1 and the hadron multiplicities in the energy range from 1.6 to 91 GeV within the errors or at least within 5%. In this description only the QCD scale Λ and a k_\perp cutoff parameter $Q_0 \gtrsim \Lambda$ for the hadrons according to the LPHD picture have been adjusted to the data. The ratio of gluon to quark multiplicity at LEP-1 is described as well.

Of particular interest is the success of this model in the regions where perturbative QCD is not expected to be relevant a priori, namely for small transverse momenta, where the running coupling gets large, either for the hadron multiplicity near threshold or for the jet multiplicity at very high resolution. In both cases the strong effect of the running α_s is clearly seen from the comparison of the two multiplicities at the same scale y_c ; taking the transverse momentum as the argument of α_s provides about the right separation. It appears that perturbative QCD is still successful in these extreme kinematic regions for this inclusive quantity.

The model for hadron production emerging from this analysis is very simple. A hadron can be treated formally like a narrow microjet of partons but with the radiated partons being so soft ($\Lambda < k_\perp < Q_0$) that they cannot be resolved and are therefore confined in a region characterized by the hadronic scale Q_0 of a few hundred MeV. So a hadron in this picture does not correspond to a colour singlet state of “valence partons” but rather to a single parton (quark or gluon) with about the same momentum together with a “sea” of soft confined partons which take care of the colour neutralization. In this way the soft hadronization picture can become consistent with the perturbative treatment of particle production.

References

- [1] A. Bassetto, M. Ciafaloni and G. Marchesini, Phys. Lett. **B83** (1979) 207.
- [2] Yu. L. Dokshitzer, V. A. Khoze, A. H. Mueller and S. I. Troyan, Rev. Mod. Phys. **60** (1988) 373; “Basics of Perturbative QCD”, ed. J. Tran Thanh Van, Editions Frontières, Gif-sur-Yvette, 1991.
- [3] Ya. I. Azimov, Yu. L. Dokshitzer, V. A. Khoze and S. I. Troyan, Z. Phys. **C27** (1985) 65 and **C31** (1986) 213.
- [4] OPAL Coll., M. Z. Akrawy et al., Phys. Lett. **B247** (1990) 617.
- [5] S. Lupia and W. Ochs, Phys. Lett. **B365** (1996) 339; preprint MPI-PhT/97-26 (hep-ph/9704319), “Low and High Energy Limits of Particle Spectra in QCD-jets”, to appear in Z. Phys. C.
- [6] G. Kramer and B. Lampe, Fortschr. Phys. **37** (1989) 161; Z. Phys. **C34** (1987) 497; Z. Phys. **C39** (1988).
- [7] Report of the Hard QCD Working Group: W. J. Stirling, J. Phys. **G17** (1991) 1567.
- [8] N. Brown and W. J. Stirling, Phys. Lett. **B252** (1990) 657; Z. Phys. **C53** (1992) 629.
- [9] S. Catani, Yu. L. Dokshitzer, M. Olsson, G. Turnock and B. R. Webber, Phys. Lett. **B269** (1991) 432.
- [10] S. Catani, Yu. L. Dokshitzer, F. Fiorani and B. R. Webber, Nucl. Phys. **B377** (1992) 445.
- [11] Yu. L. Dokshitzer and M. Olsson, Nucl. Phys. **B396** (1993) 137.
- [12] L3 Collaboration: O. Adriani et al., Phys. Lett. **B284** (1992) 471.
- [13] OPAL Collaboration: R. Acton et al., Z. Phys. **C59** (1993) 1.
- [14] V.A. Khoze and W. Ochs, Int. J. Mod. Phys. **A12** (1997) 2949.
- [15] Yu. L. Dokshitzer and S. I. Troyan, Proc. 19th Winter School of the LNPI, Vol. 1, p.144; Leningrad preprint LNPI-922 (1984).
- [16] G. Altarelli and G. Parisi, Nucl. Phys. **B126** (1977) 298; Yu. L. Dokshitzer, Sov. Phys. JETP, **46** (1977) 641.

- [17] Yu. L. Dokshitzer, V. A. Khoze and S. I. Troyan, *Int. J. Mod. Phys. **A7*** (1992) 1875.
- [18] ADONE Coll., B. Esposito et al., *Lett. Nuovo Cimento **19*** (1977) 21; MARK I Coll., J. L. Siegrist et al., *Phys. Rev. **D26*** (1982) 969; JADE Coll., W. Bartel et al., *Z. Phys. **C20*** (1983) 187; PLUTO Coll., C. Berger et al., *Phys. Lett. **B95*** (1980) 313; TASSO Coll., W. Braunschweig et al., *Z. Phys. **C45*** (1989) 193; TPC/2 γ Collaboration: H. Aihara et al., *Phys. Lett. **B134*** (1987) 299; HRS Coll., M. Derrick et al., *Phys. Rev. **D34*** (1986) 3304; TOPAZ Coll., M. Yamauchi et al., *Proc. XXIV Int. Conf. on High Energy Physics* (Munich, 1988), Springer Verlag, Eds. R. Kotthaus and J. H. Kühn, p. 852; AMY Coll., H. W. Zheng et al., *Phys. Rev. **D42*** (1990) 737; ALEPH Coll., D. Decamp et al., *Phys. Lett. **B273*** (1991) 181; DELPHI Coll., P. Abreu et al., *Z. Phys. **C50*** (1991) 185; OPAL Coll., D. Acton et al., *Z. Phys. **C53*** (1992) 539; L3 Coll., B. Adeva et al., *Z. Phys. **C55*** (1992) 39; MARKII Coll., G. S. Abrams et al., *Phys. Rev. Lett. **64*** (1990) 1334.
- [19] V. A. Khoze, S. Lupia and W. Ochs, *Phys. Lett. **B394*** (1997) 179
- [20] CLEO Coll., M. S. Alam et al., *Phys. Rev. **D56*** (1997) 17.
- [21] J. W. Gary, *Phys. Rev. **D49*** (1994) 4503.
- [22] OPAL Coll., G. Alexander et al., *Phys. Lett. **B388*** (1996) 659.
- [23] J. Fuster, S. Cabrera and S. Marti i Garcia, *Nucl Phys. **B54A*** (Proc. Suppl.) (1997) 39.
- [24] S. J. Brodsky and J. F. Gunion, *Phys. Rev. Lett. **37*** (1976) 402.
- [25] A. H. Mueller, *Nucl Phys. **B241*** (1984) 141; E. D. Malaza, B. R. Webber, *Phys. Lett. **B149*** (1984) 501; *Nucl. Phys. **B267*** (1986) 70.
- [26] J. B. Gaffney and A. H. Mueller, *Nucl. Phys. **B250*** (1985) 109.
- [27] I. M. Dremin and V. A. Nechitailo, *Mod. Phys. Lett. **A9*** (1994) 1471; I. M. Dremin and R. C. Hwa, *Phys. Lett. **B324*** (1994) 477.

Figure Captions

Fig. 1a: Data on the average jet multiplicity at $Q = 91$ GeV[12,13] and the average hadron multiplicity (assuming $\mathcal{N} = \frac{3}{2}\mathcal{N}_{ch}$) at different *cms* energies[18] with $Q_c = 0.507$ GeV as a function of y_c . The solid (dashed) line shows the prediction in absolute normalization for the hadron (jet) multiplicity obtained by using eq. (12) with parameters from eq. (13). The right most data point for hadrons ($Q_0 = 1.6$ GeV) refers to pions only.

Fig. 1b: Data as in Fig. 1a, but $\mathcal{N} - 2$ is now shown. The solid lines show the complete predictions of eq. (12) for both the particle and jet multiplicities, the dashed lines the contribution of eq. (5) alone. The same parameters as in Fig. 1a are used.

Fig. 2: Data on the ratio of average hadron multiplicities in quark and gluon jets at $y_c \sim 3 \times 10^{-5}$ from OPAL[22] and around $y_c \sim 0.01$ from CLEO[20] with $Q_c = 0.507$ GeV as a function of y_c . The solid (dashed) line shows the prediction for the ratio of hadron (jet) multiplicities in quark and gluon jets obtained by using eq. (5) with the same parameters as in Fig. 1.

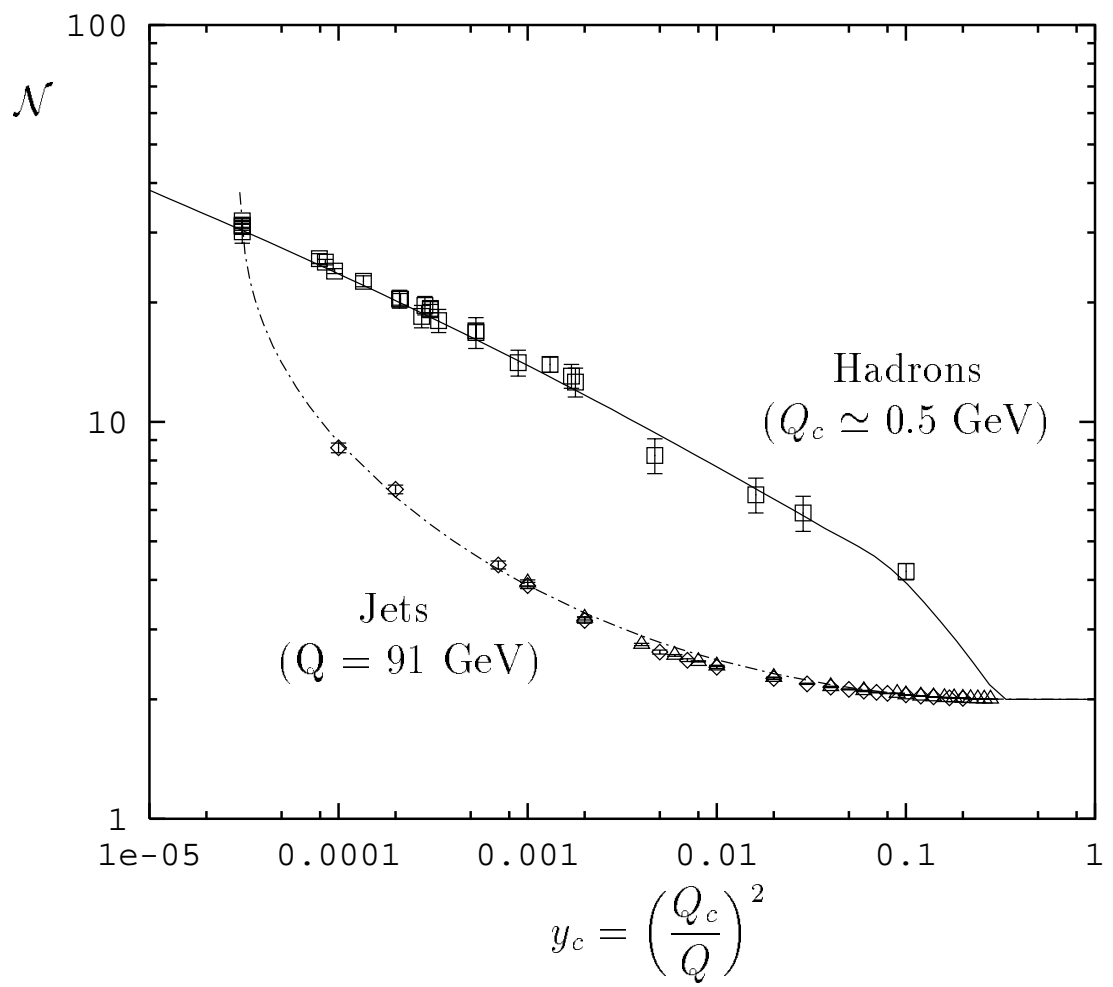


Figure 1: a

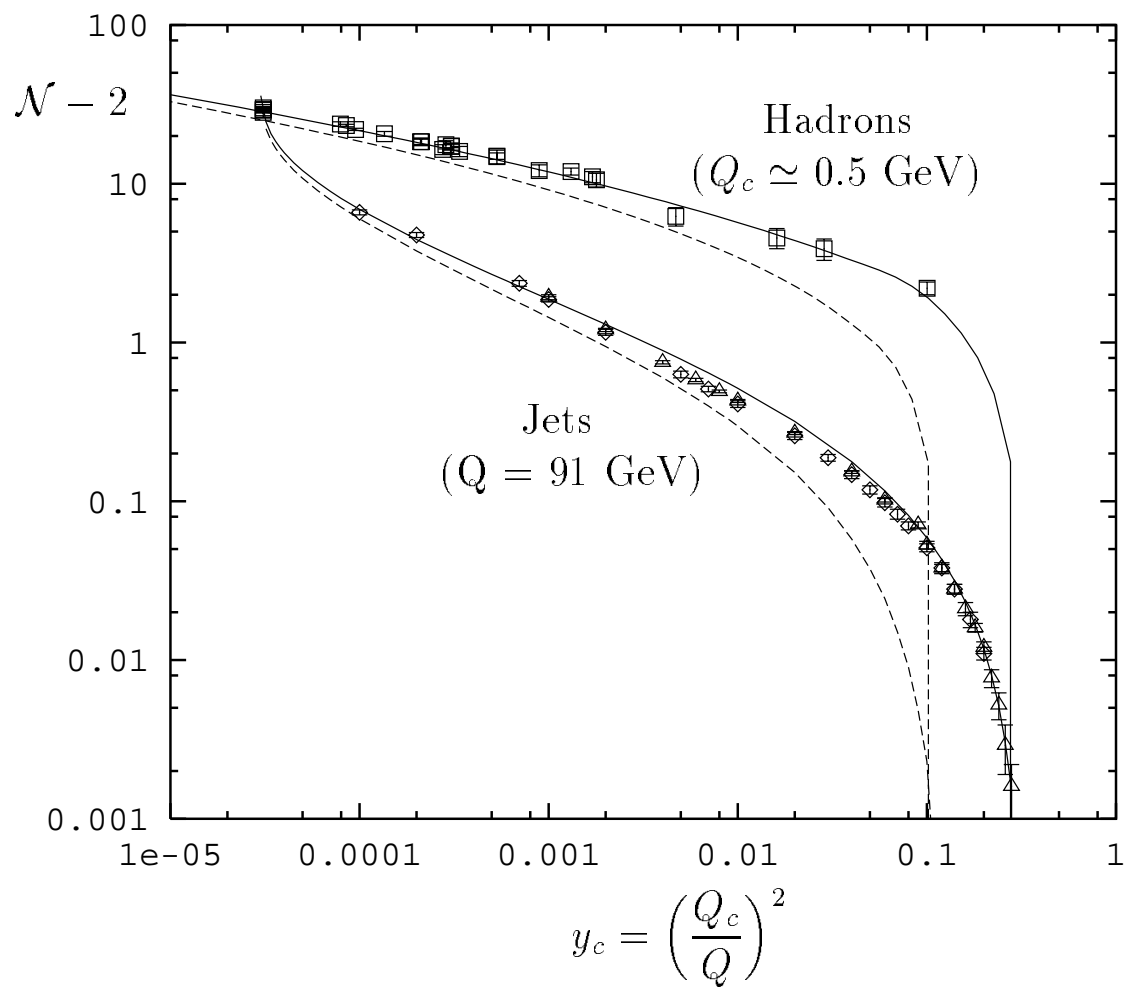


Figure 1: b

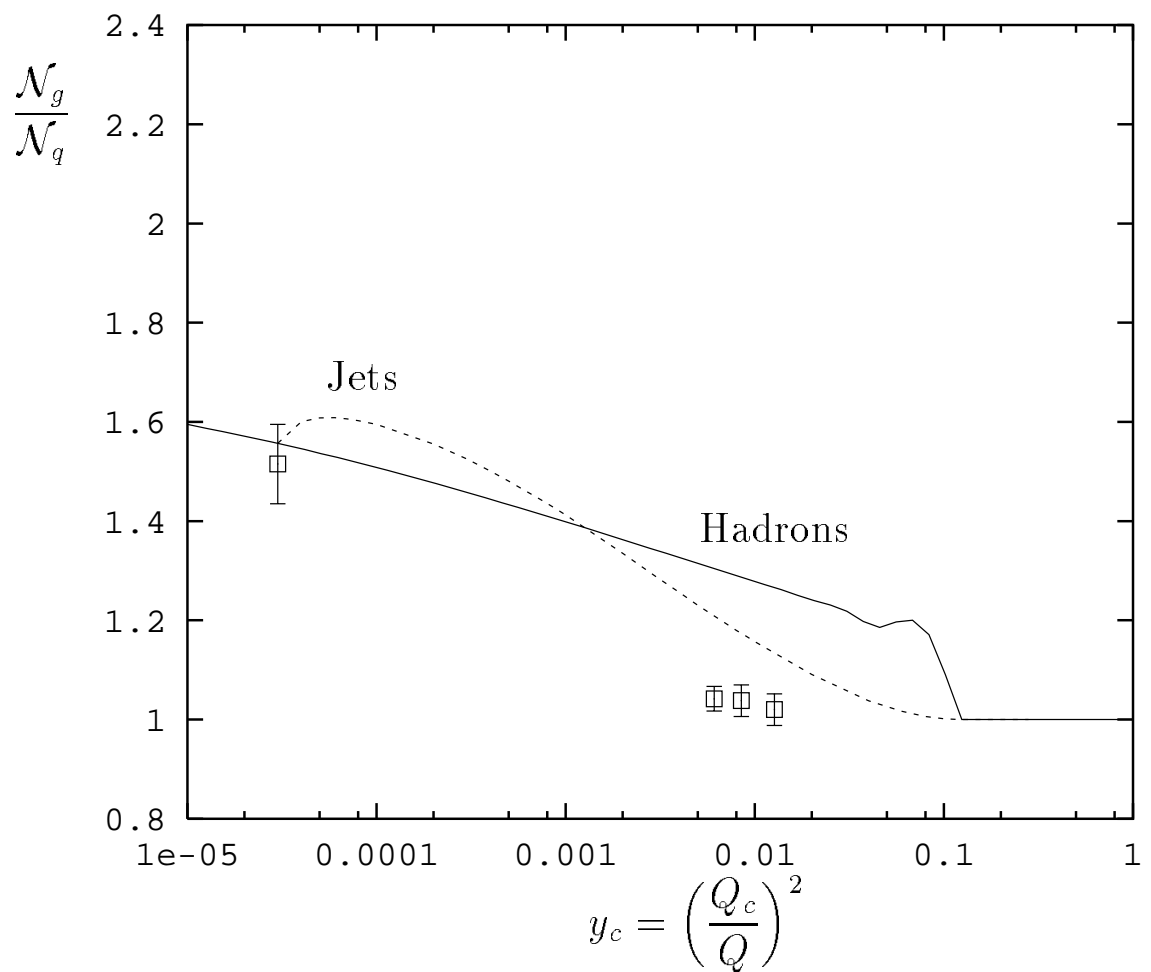


Figure 2: